2015 IEEE International Conference on Robotics and Automation (ICRA)
Washington State Convention Center
Seattle, Washington, May 26-30, 2015

Design of a Cable-driven Active Leg Exoskeleton (C-ALEX) and Gait Training Experiments with Human Subjects

Xin Jin, Xiang Cui and Sunil K. Agrawal*

Abstract— **Robotic rehabilitation devices are attractive to physical therapists. Various leg exoskeletons have been developed during the past decade and have been used in gait training. Traditional exoskeletons usually have a complex structure and add extra inertia to the wearer's leg, which may change their natural gait. In this paper, we present the design of a cable-driven active leg exoskeleton (C-ALEX) for human gait training. The advantages of cable-driven designs are that they have a simpler structure, add minimal inertia to the human limbs, and do not require precise joint alignment. C-ALEX employs the "assist-as-needed" control strategy to help the ankle center move along a prescribed path. An experiment with 6 healthy subjects was conducted who walked with C-ALEX on a treadmill. The results showed that C-ALEX is capable of helping the subjects better track a prescribed ankle path.**

I. Introduction

Robotic rehabilitation devices have gained high popularity in physical therapy. The advantages of robotic rehabilitation devices include their ability to offer uniform training over long time and across different groups. They can provide quantitative measures of the subject's performance and the required labor of physical therapists can be greatly reduced [1].

Various leg exoskeletons have been developed for gait training of neurologically impaired patients. Among these are Lokomat from Hocoma AG [2], LOPES [3] and Shadow Leg [4] from University of Twente, and ALEX I, II and III [6], [7] from our group. These exoskeletons have gone through extensive testing both with healty subjects [3], [6] and with stroke patients [2], [5] and produced favorable results. These studies have shown that gait training exoskeletons can improve the gait of neurologically impaired patients.

Traditional leg exoskeletons such as Lokomat or ALEX use links and mechanical joints placed in parallel with human limbs and joints. The mechanical structure adds extra weight and inertia to the human limbs which changes the natural walking dynamics of the wearer. Furthermore, accurate alignment between the joints of the exoskeleton and the wearer is required which is hard to accomplish due to the complex geometry of the human body. Some exoskeletons try to reduce the moving inertia and the need for accurate alignment [4], [8] at the cost of a more complicated mechanical structure.

X. Jin and S.K. Agrawal* are with the Department of Mechanical Engineering, Columbia University, New York, NY, USA x.jin and sunil.agrawal@columbia.edu

X. Cui is with the School of Automation Science and Electrical Engineering, Beihang University, Beijing, China

*Corresponding author

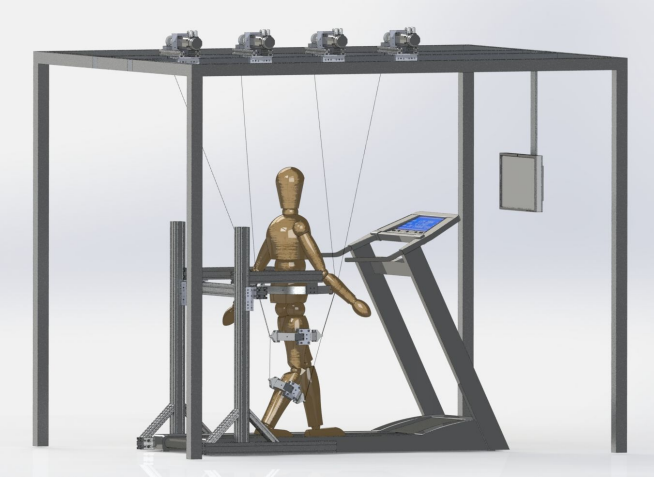

Fig. 1. An illustration of a wearer walking with the Cable-drive Active Leg EXoskeleton (C-ALEX) on a treadmill.

Cable-driven designs have been used in only a few rehabilitation devices. Vashista et al. demonstrated A-TPAD that uses cables to apply force to wearer's waist during treadmill walking [9]. Wu et al. designed a cable-driven device named CaLT for gait training with spinal cord injury patient [10] and obtained desirable experimental results. However, CaLT was an end-effector type device in which cables are directly attached to the ankle of the wearer, and therefore can only apply force at the ankle level. Mao et al. proposed a cable-driven arm exoskeleton CAREX for rehabilitation training of the arm [11]. CAREX has cuffs on the shoulder, upper-arm and forearm and routes cables through these segments. CAREX does not have rigid links and mechanical joints, thus, has the advantage of being light weight and low moving inertia. Additionally, no joint alignment is required within CAREX. It has been shown to be effective in improving the performance of path tracking tasks among healthy subjects [12].

In this paper, we extend the idea of cable-driven designs to the lower extremity and present the design of a Cable-driven Active Leg EXoskeleton (C-ALEX) for gait training. The exoskeleton comprises of three cuffs connected to the waist, thigh and shank of the wearer, with cables routed through them. No rigid link or joint is used within the exoskeleton. The exoskeleton is controlled in force mode using an assist-as-needed control paradigm. An experiment with 6 subjects was carried out which shows that C-ALEX can effectively assist its wearer to alter his or her gait.

978-1-4799-6923-4/15/$31.00 ©2015 IEEE

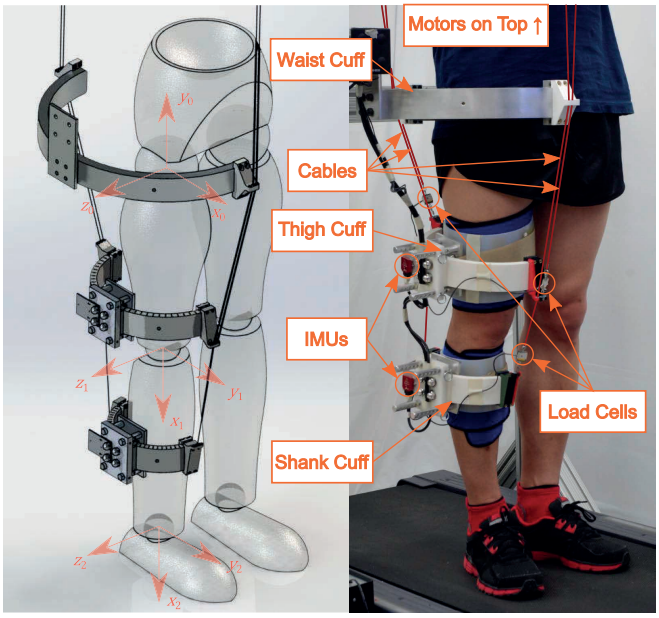

Fig. 2. The picture on the right is C-ALEX attached to a subject's leg. The picture on the left is a CAD model of the exoskeleton with local coordinate system for each segment of the leg.

II. Design of C-ALEX

A. Exoskeleton Design

Fig. 2 shows a subject wearing C-ALEX. The exoskeleton mainly consists of three cuffs: the waist cuff, the thigh cuff and the shank cuff. The waist cuff is fixed to a height-adjustable external support frame. The thigh and the shank cuffs are tightly connected to the wearer's thigh and shank, respectively. To create a secure connection between the thigh and shank cuffs and the leg, a layer of medical bondage is first placed on to the subject's leg. An orthotics with velcro liners is then strapped on top of the medical straps. The cuffs are attached at the lateral side of the orthotics. The lateral distance between the cuff and the leg can be adjusted. To reduce the weight of the exoskeleton on subject's leg, the thigh and shank cuffs are primarily made of 3D printed ABS plastic with sparse interior. The overall weight of the thigh and shank cuffs are 0.60kg and 0.54kg, respectively.

Four cables are used to actuate the exoskeleton. The cables are pre-stretched Nylon coated steel wires. All four cables are routed through the waist cuff. Two of these are attached to the thigh cuff, and the other two are routed through the thigh cuff and attached to the shank cuff. These four cables actuate two degrees-of-freedom of the wearer's leg: the hip flexion/extension and the knee flexion/extension. The DH parameters of the exoskeleton are shown in Table I. In the DH parameters, q_1 is the hip flexion angle and q_2 is the knee flexion angle. L_{th} stands for thigh length, and L_{sh} stands for shank length. These two parameters vary between individuals, and therefore need to be measured and provided for each subject. The kinematics of C-ALEX are derived through the DH parameters and homogeneous transformations. All the cable routing points on the cuff have Teflon liners to reduce the friction between the cable and the cuff. The cable routing points are designed to be able to slide along the cuff to change the cable routing. Additional cable routing points can be added to accommodate extra cables to increase the controlled degrees-of-freedom.

TABLE I
DH Parameters

Link	a	d	α	θ
1	L_{th}	0	0°	$q_1 - 90°$
2	L_{sh}	0	0°	$-q_2$

B. Actuation and Control System

Each cable in the exoskeleton is driven by a Kollmorgen AKM43 servo motor with custom made cable reels. The cable reels are used to help proper winding of the cables. The motors are powered by Kollmorgen AKM servo drives operating in torque mode. To measure the tension in the cables, a load cell is connected to the end of each cable. The load cells are Futek LSB200 with CSG110 signal conditioners. There is a VectorNav VN-100 inertia measurement unit (IMU) mounted on the thigh cuff and shank cuff to measure the hip and knee angle of the wearer during walking. A National Instrument PXIe-8135 controller is used for real-time control and data acquisition of the exoskeleton. The controlling software is developed in LabVIEW.

C. Dynamical Model of the Robotic Leg

The dynamic equations of motion of C-ALEX are derived through the Lagrangian method in Mathematica. The generalized coordinates q_1 and q_2 represent the angle of hip flexion and knee flexion, respectively. The equations of motion take the following form:

$$D(q)\ddot{q} + C(q,\dot{q})\dot{q} + G(q) = U, \tag{1}$$

where $q = [q_1, q_2]^T$ is the vector of generalized coordinates; $D(q)$ is the 2×2 inertia matrix; $C(q,\dot{q})$ is the vector of Coriolis and centripetal terms; $G(q)$ is the vector of gravity terms; U is the vector of generalized force corresponding to the generalized coordinates q. The left hand side of (1) closely resembles the dynamical equation of a double pendulum. The geometric and inertial parameters in (1) were obtained through the CAD model of C-ALEX and measurements from the wearer's leg. The generalized force U on right hand side of (1) is the torque at the hip and knee joint generated by the cables. The relation between the joint torque U and the cable tension T can be obtained by the virtual work principle.

Fig. 3 shows the schematic of a two-link system actuated by a single cable. A force T is applied on the cable which results in the configuration of the two-link system to change. We will use the principle of virtual work to generate the input-output mapping between the cable tension T and the vector U in (1). The tension T will result in the cable to be pulled out by l. From the principle of virtual work, we have:

$$\delta W = T \cdot \delta l = U \cdot \delta q, \tag{2}$$

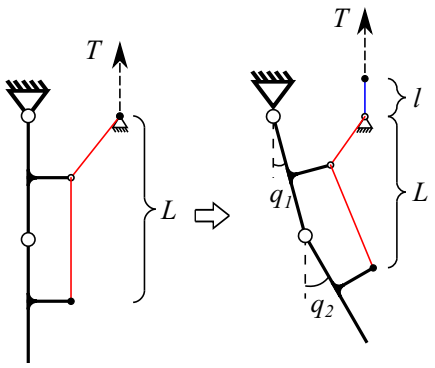

Fig. 3. A schematic of a two link system actuated by a single cable. l denotes the cable pulled out by force T, and L denotes the cable that remains in the system.

where U and q are the generalize forces and coordinates (i.e. joint torques and joint angles). We also have

$$\delta l = \frac{\partial l}{\partial q}\,\delta q. \tag{3}$$

Using L to denote the length of cable that remains in the system, it is apparent that $l + L = constant$ (total length of the cable is constant), which gives:

$$\frac{\partial L}{\partial q} + \frac{\partial l}{\partial q} = 0\,. \tag{4}$$

Substituting (3) and (4) into (2), the relationship between the joint torque U and the cable tension T can be formulated as:

$$U = -(\frac{\partial L}{\partial q})^T\,T = J_T(q)^T\,T\,. \tag{5}$$

With 4 cables within C-ALEX, the Jacobian matrix $J_T(q)$ can be written as

$$J_T(q) = -\frac{\partial(L_1, L_2, L_3, L_4)}{\partial(q_1, q_2)}\,, \tag{6}$$

where L_i is the length of cable i measured from the routing point on the waist cuff to the final attachment point of the cable on the thigh or shank cuffs.

Equation (5) is of particular importance to the system as it provides the foundation to solve for the required cable tensions when some specific torques are desired at the joints.

D. Cable Tension Planning

In order for the exoskeleton to generate a set of torques at the joints, we must calculate the tensions to be applied by the motors on the cables. When torque U is required at the joints, cable tension T can be found by solving the set of linear equations:

$$J_T(q)^T\,T = U\,, \tag{7}$$

where $J_T(q)$ is the Jacobian matrix in (6), U is the vector of torques we would like the exoskeleton to generate at the joints, and T is the vector of cable tensions we need to solve.

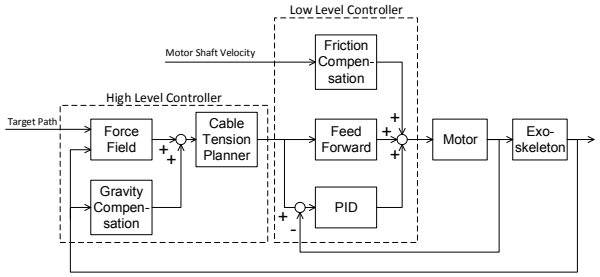

Fig. 4. A block diagram for the controller of C-ALEX

Equation (7) is underdetermined as the number of cables is larger than the degrees-of-freedom of the system.

The range of tensions in the cables is limited. Since cables can only pull but not push, it is impossible for the tensions in the cables to be negative. In the actual system, due to the existence of friction along the cables, the minimum tension in a cable needs to be set above a positive value to keep the cable taut. Also, because the motors connected to the cables can only produce limited torque, there is a maximum limit on cable tensions as well. Therefore, T should satisfy:

$$T \in [T_{min}, T_{max}]\,. \tag{8}$$

In the case of C-ALEX, the cable tension range is set in between 7N and 70N.

Using (7) and (8) as constraints, an optimization problem can be formulated to find a proper set of cable tensions to generate desired torques. We use a quadratic objective function: $f(T) = T^T\,T$ for the optimization problem, which minimizes the norm of cable tension vector. The advantage of using quadratic programming over linear programming is that the solution to T will change more continuously when the Jacobian matrix $J_T(q)$ in the equality constraint (7) changes. This will help to avoid abrupt cable tension changes when the leg moves from one configuration to another.

Overall, the cable tension planning problem can be formulated into this quadratic programming problem:

$$\min f(T) = T^T\,T$$
$$\text{s.t.} \quad J_T(q)^T \cdot T = U \quad \text{and} \quad T \in [T_{min}, T_{max}]\,.$$

LabVIEW provides a quadratic programming solver that uses the active set method. This solver is used to solve the above problem in real time. The disadvantage of quadratic programming is that it is time consuming to solve. However, our controller is capable of solving the above problem at 100Hz without any delay.

III. Controller of the Exoskeleton

This exoskeleton is aimed at rehabilitation and therefore the controller uses an "assist-as-needed" strategy. The goal of the controller is to assist the ankle point of the wearer of the exoskeleton to move on a prescribed target path. The controller creates a tunnel-like force-field around the target path. If the end effector (ankle point) deviates from the target

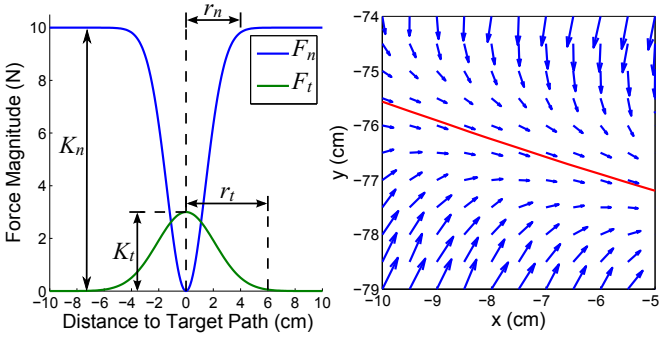

Fig. 5. The left figure shows the magnitude of the force field as a function of the normal distance to the target path. The blue line shows the normal component and the green line shows the tangential component of the force field. The right figure shows a portion of the force field around a target path. The red line is the target path, and the blue arrows show the directions and magnitudes of the force field.

path, the controller acts as a spring and pulls the end effector back to the target path. A two-level controller is implemented as shown in Fig. 4: A high level force-field controller that uses the position feedback of the exoskeleton to dictate the necessary cable tensions to create the force field, and a low level cable tension controller that controls the motors to produce the desired cable tensions using feedback from the load cells on the cables.

The high level force-field controller generates a force F at the ankle point that has two components:

$$F = F_n + F_t. \tag{9}$$

F_n is normal to the target path, and it will push the ankle point closer to the path. F_t is tangential to the target path, pointing to the direction of movement, and it provides a gentle push to move the ankle point along the target path. The magnitude of F_n, F_t is calculated as:

$$\begin{aligned} \|F_n\| &= K_n \cdot (1 - e^{-(\frac{2d}{r_n})^2}) \\ \|F_t\| &= K_t \cdot e^{-(\frac{2d}{r_t})^2}, \end{aligned} \tag{10}$$

in which K_n and K_t are the gains of the force field, d is the distance from the ankle point to its nearest point on the target path. Equation (10) effectively creates two tunnels around the target path with diameters of r_n and r_t respectively. For the normal force F_n, the magnitude roughly equals to K_n outside the tunnel and gradually deceases to 0 inside the tunnel. For the tangential force F_t, the magnitude is 0 outside the tunnel and gradually increases to K_t inside the tunnel. Fig. 5 shows the change of F_n and F_t as a function of the normal distance from the target path d, and a qualitative sketch of the force field around a target path.

The force-field controller has two modes: the transparent mode and the force-field mode. The transparent mode is used for collecting the natural gait of the wearer. In the transparent mode, C-ALEX will try to minimize its interaction with the wearer. It will only balance its own weight and will not provide any assistance. Therefore, the required joint torque U in the transparent mode is simply:

$$U = G(q)\,, \tag{11}$$

in which $G(q)$ is the gravity terms in (1). The force-field mode is used for assisting the wearer to track the target ankle path. In the force-field mode, C-ALEX generates the aforementioned force field besides compensating for its own weight. The required joint torque U in the force-field mode can be found by:

$$U = J_e(q)^T F + G(q)\,, \tag{12}$$

where F is the force-field force in (10) and $J_e(q)$ is the Jacobian matrix of the end effector.

With the required joint torque U obtained, the force-field controller uses the cable tension planning detailed in Section II-D to calculate the desired tension for each cable and send it to the low level controller.

The low level controller includes three parts: A feed-forward part using the motor constant, a friction compensation part using the motor's friction-speed model, and a close loop PID controller using the feedback from the load cells in the cables. Together, the low level controller is able to control the motors to generate tensions that closely follow the desired tensions calculated from the high level controller.

IV. Evaluation of C-ALEX on Healthy Subjects

An experiment was conducted to evaluate the performance of C-ALEX. The goal of the experiment was to verify that C-ALEX with the force field controller can assist the wearer to track a target ankle path different from his or her natural path. In the experiment, the subjects tracked a target ankle path with C-ALEX in both the force-field mode and the transparent mode. The hypothesis is that subjects will have better path tracking performance in the force-field mode than in the transparent mode.

The setup of the experiment is shown in Fig. 6. Six healthy subjects participated in the experiment. The subjects were all male, aged between 20 and 35 years. Fig. 7 shows the protocol of the experiment. At the beginning of each experiment, C-ALEX was fitted onto the right leg of the subject, and then the experimenter took measurements of the length of the thigh and the shank of the subject as well as the locations of the cuffs. These measurements were provided to the controller. Each experiment was divided into 4 sessions: the familiarization session, the baseline session, the force-field (FF) session and the transparent (TR) session. Each session was 4 minutes long, and a 2 minutes break was given between each session.

The experiment started with the familiarization session, during which C-ALEX was put into the transparent mode. The subject was instructed to walk on a treadmill to get familiar with walking with C-ALEX. The speed of the treadmill was adjusted to the comfortable walking speed of the subject. Following the familiarization session was the baseline session, during which C-ALEX stayed in the transparent mode. The subject was instructed to walk naturally during this session. The natural gait pattern collected during

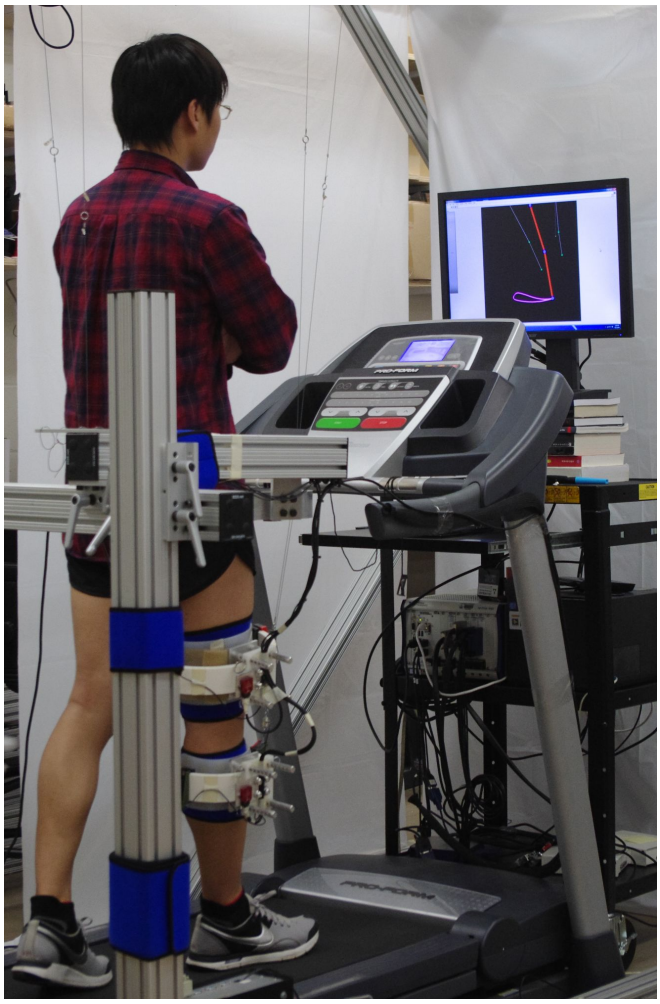

Fig. 6. This figure shows the experimental set up to evaluate C-ALEX. The subject was wearing C-ALEX and walking on a treadmill. The screen in front of the subject was displaying the motion of the subject's right leg in sagittal plane as well as the target ankle path for the subject to follow.

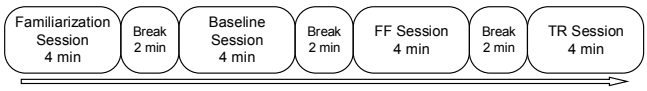

Fig. 7. The protocol of the experiment

this session was later used to generate the target ankle path in the FF and the TR sessions. The screen in front of the subject was turned off during the first two sessions.

During the baseline session, the hip and knee joint angles and the ankle path were recorded. Data during the first and the last minutes were discarded, and the remaining data were cut into gait cycles at the anterior most point of the ankle path and averaged across the gait cycles to obtain the averaged joint angles in a single gait cycle. The averaged joint angles were then reduced by 20% to create an ankle path that is both shorter and shallower than the baseline path. The top figure of Fig. 8 shows the baseline ankle path (black) and the modified ankle path (red) from a representative subject.

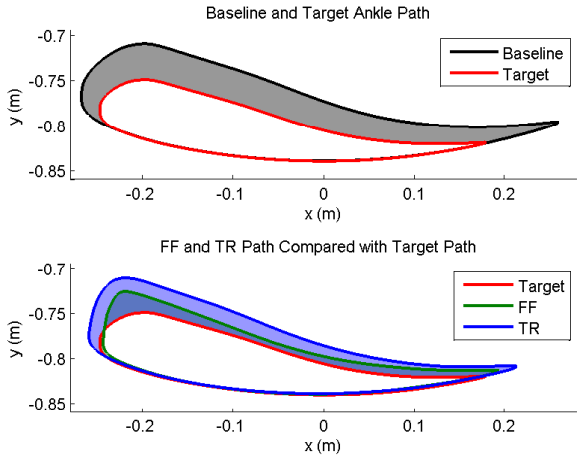

Fig. 8. Ankle path from a representative subject. The grey shaded area in the top figure is the deviation area between the baseline path and the target path. The blue and the green shaded areas in the bottom figure are the deviation area of the TR path and the deviation area of FF path, respectively.

This modified ankle path was then used as the target ankle path in the FF and the TR sessions.

During the FF and the TR sessions, the screen in front of the subject was turned on to display the current configuration of the leg and the target ankle path, as shown in Fig. 6. The subject was instructed to try to walk as closely to the target path as possible during these two sessions. During the FF session, C-ALEX was put into the force-field mode. The force-field gains in (9) were set as $K_n = 20, r_n = 0.1, K_t = 3, r_t = 0.05$ and were consistent across all subjects. After FF session was the TR session, during which C-ALEX was put into the transparent mode. After the experiment, the joint angles and ankle path during each session were analyzed.

The ankle path during the FF and the TR sessions were recorded, cut and averaged the same way as the ankle path during the baseline. The average ankle path during the FF and the TR sessions of the same representative subject was plotted in the bottom figure of Fig. 8. It can be observed from the figure that the FF path is closer to the target path than the TR path, which demonstrates the effectiveness of the force-field controller of C-ALEX.

To quantify the effectiveness of C-ALEX, the normalized error area (NEA) [7] of the FF path and the TR path was calculated and compared. Fig. 8 shows the deviation area of the baseline path (gray shaded area), the deviation area of the FF path (green shaded area) and the deviation area of the TR path (blue shaded area). The NEA of the FF(TR) path is calculated as the ratio between the deviation area of the FF(TR) path and the deviation area of the baseline path, i.e. the green(blue) shaded area divided by the grey shaded area. A smaller NEA suggests that the path closely overlaps the target path. Fig. 9 shows the average NEA from all subjects. The average NEA in the FF sessions is 0.493 ± 0.421 (mean$\pm$SD), and the average NEA in the TR sessions is 0.751 ± 0.572 (mean$\pm$SD). As we have only 6

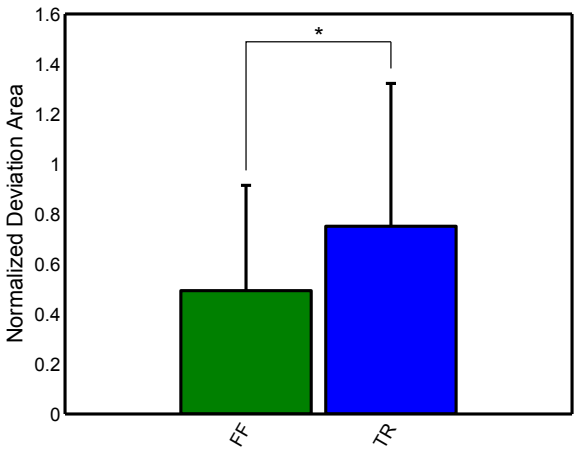

Fig. 9. The mean and standard deviation of NEA in FF sessions and TR sessions. "$*$" indicates a statistically significant difference ($p = 0.031$).

subjects, we used the Wilcoxon signed rank test to evaluate the difference between the NEA in FF sessions and the NEA in TR sessions. The result shows that the NEA in FF sessions is significantly smaller than that in TR sessions ($p = 0.031$). This result validates our hypothesis that C-ALEX with force field can help the subject to follow a prescribed ankle path.

V. Conclusion and Future Work

In conclusion, this paper presented the design of a Cable-driven Active Leg EXoskeleton (C-ALEX) for human gait training. The exoskeleton is controlled by a force-field controller, which is able to assist the motion of the leg and help the ankle to follow a desired path. An experiment with six subjects wearing C-ALEX was performed to validate the device and the controller. The results showed that the force-field controller is able to help the subject better tracking a prescribed ankle path.

The current design of C-ALEX has some limitations which are currently being addressed: (i) the waist cuff of the exoskeleton is fixed to the ground, which restricts the pelvic motion of the wearer; (ii) the current cable routing can only provide assistive force in the sagittal plane; (iii) the locations of the cuffs have to be measured manually, which brings some inaccuracy. To solve these problems, we are currently designing a new waist cuff that can be worn by subjects, thus eliminating the need for a fixed support. With the new waist cuff, a new cable routing will be used that can generate assistive hip abduction/adduction torques as well. We will also use measurements of cable lengths to better estimate the cuff locations. A training experiment will be conducted after these improvements are made to evaluate how subjects will learn and retain their new trajectories after walking in C-ALEX with force field.

Acknowledgment

This work was supported by the the National Robotics Initiative program from National Science Foundation under grant NSF IIS-1339666.

References

[1] A. Pennycott, D. Wyss, H. Vallery, V. Klamroth-Marganska, and R. Riener, "Towards more effective robotic gait training for stroke rehabilitation: a review," *Journal of NeuroEngineering and Rehabilitation*, vol. 9, p. 65, Sept. 2012.

[2] R. Riener, L. Lnenburger, I. Maier, G. Colombo, and V. Dietz, "Locomotor training in subjects with sensori-motor deficits: An overview of the robotic gait orthosis lokomat," *Journal of Healthcare Engineering*, vol. 1, pp. 197–216, June 2010.

[3] J. Veneman, R. Kruidhof, E. E. G. Hekman, R. Ekkelenkamp, E. H. F. Van Asseldonk, and H. van der Kooij, "Design and evaluation of the LOPES exoskeleton robot for interactive gait rehabilitation," *IEEE Transactions on Neural Systems and Rehabilitation Engineering*, vol. 15, pp. 379–386, Sept. 2007.

[4] J. Meuleman, E. van Asseldonk, and H. van der Kooij, "Novel actuation design of a gait trainer with shadow leg approach," in *2013 IEEE International Conference on Rehabilitation Robotics (ICORR)*, pp. 1–8, June 2013.

[5] S. Srivastava, P. Kao, S. Kim, P. Stegall, D. Zanotto, J. Higginson, S. Agrawal, and J. Scholz, "Assist-as-Needed Robot-Aided Gait Training Improves Walking Function in Individuals Following Stroke," in *IEEE Transactions on Neural Systems and Rehabilitation Engineering*, vol. PP, no. 99, pp. 1–1, 2014.

[6] P. Stegall, K. Winfree, D. Zanotto, and S. Agrawal, "Rehabilitation exoskeleton design: Exploring the effect of the anterior lunge degree of freedom," *IEEE Transactions on Robotics*, vol. 29, pp. 838–846, Aug. 2013.

[7] D. Zanotto, P. Stegall, and S. K. Agrawal, "Adaptive assist-as-needed controller to improve gait symmetry in robot-assisted gait training," in *2014 IEEE International Conference on Robotics and Automation (ICRA)*, pp. 724–729, May 2014.

[8] D. Zanotto, P. Stegall, and S. Agrawal, "ALEX III: A novel robotic platform with 12 DOFs for human gait training," in *2013 IEEE International Conference on Robotics and Automation (ICRA)*, pp. 3914–3919, May 2013.

[9] V. Vashista, X. Jin, and S. K. Agrawal, "Active tethered pelvic assist device (a-TPAD) to study force adaptation in human walking," in *2014 IEEE International Conference on Robotics and Automation (ICRA)*, pp. 718–723, May 2014.

[10] M. Wu, T. G. Hornby, J. M. Landry, H. Roth, and B. D. Schmit, "A cable-driven locomotor training system for restoration of gait in human SCI," *Gait & Posture*, vol. 33, pp. 256–260, Feb. 2011.

[11] Y. Mao and S. K. Agrawal, "Design of a cable-driven arm exoskeleton (CAREX) for neural rehabilitation," *IEEE Transactions on Robotics*, vol. 28, pp. 922–931, Aug. 2012.

[12] Y. Mao, X. Jin, G. Dutta, J. Scholz, and S. Agrawal, "Human movement training with a cable driven ARm EXoskeleton (CAREX)," *IEEE Transactions on Neural Systems and Rehabilitation Engineering*, vol. 23, no. 1, pp. 84-92, Jan. 2015.